Weak anisotropic x-ray magnetic linear dichroism at the Eu $M_{4,5}$ edges of ferromagnetic EuO(001): Evidence for $4f$-state contributions

Gerrit van der Laan,[1,2] Elke Arenholz,[3] Andreas Schmehl,[4] and Darrell G. Schlom[5]

[1]*Magnetic Spectroscopy Group, Daresbury Laboratory,*
Warrington WA4 4AD, United Kingdom
[2]*Diamond Light Source, Chilton, Didcot,*
Oxfordshire OX11 0DE, United Kingdom
[3]*Advanced Light Source, Lawrence Berkeley National Laboratory, Berkeley, CA 94720*
[4]*Institut für Physik, Universität Augsburg, Augsburg, Germany*
[5]*Department of Materials Science and Engineering,*
Penn State University, University Park, PA 16802

(Dated: March 18, 2008)

Abstract

We have observed a weak anisotropic x-ray magnetic linear dichroism (AXMLD) at the Eu $M_{4,5}$ edges of ferromagnetic EuO(001), which indicates that the $4f$ states are not rotational invariant. A quantitative agreement of the AXMLD is obtained with multiplet calculations where the $4f$ final state is split by an effective cubic crystalline electrostatic field. The results indicate that the standard model of rare earths, where f electrons are treated as core states, is not correct and that the 4f electrons contribute weakly to the magnetic anisotropy of EuO.

The magnetism in rare-earth systems is governed by the magnetic moments of the localized $4f$ orbitals that interact indirectly through delocalized valence electrons. A wide variety of electronic, magnetic, and magneto-optical features, often displaying a striking temperature dependence, results from this correlation between localized and itinerant electrons in the $4f$ systems. The anisotropic properties of these systems, which are important for the use in applications such as magnetic storage devices, are still poorly understood despite decades of intense studies using optical spectroscopy. [1]

The magnetic anisotropy originates from the electrostatic interaction of the $4f$ charge density with the crystalline electric field (CEF) caused by the neighboring charges. An applied magnetic field of sufficient strength rotates the direction of $4f$ total angular momentum and due to the strong spin-orbit interaction the $4f$ charge density will rotate with it. This re-orientation of the $4f$ charge density in the CEF gives an increase in the electrostatic energy, resulting in the magnetic anisotropy energy. This is the so called standard model, where the $4f$ states are treated as core states [2, 3]. The question that one might ask here is the following. To what extend is the $4f$ charge density able to rotate freely in order to follow the magnetic moment, or could it be that the charge density is held back by the CEF and hybridization which couple it to the lattice? Actually, the latter situation occurs in the $3d$ transition metal group, where the relative sizes of the spin-orbit interaction and crystal field are reversed compared to the $4f$ metal group. The $3d$ orbitals are firmly coupled to the lattice, keeping the charge density fixed. In this case the magnetic anisotropy is proportional to the difference in the expectation value of the orbital moment along the different magnetization directions [4, 5], c.f., Fig. 1. Therefore if there is an energy splitting of the f states then the charge density of each of its sublevels will obtain a different angular dependence, which can lead to a pinning of the f states. A special situation arises for the half-filled shell, i.e., the f^7 configuration, in which case the spin-orbit interaction and orbital magnetic moment vanish, so that the charge density is no longer coupled to the spin and hence will not rotate with the magnetization. In this case it should be possible by rotating the crystal to detect the CEF anisotropy arising from the energy splitting in the $4f$ states using some suitable form of spectroscopy.

Although values of the crystal field parameters for the $4f$ states can be found in the literature, they are better known for the $5d$ states of the rare earths, where they are several eV large and obtained from $4f$ to $5d$ optical spectroscopy or magnetization measurements.
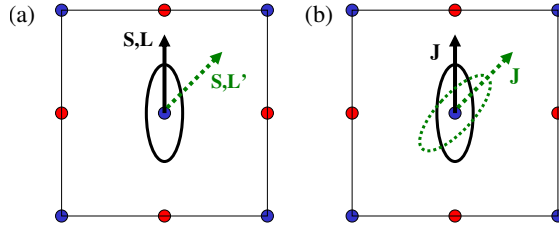
FIG. 1: (Color online) Schematics of the magnetic anisotropy for two extreme cases. (a) In $3d$ systems, where the crystalline electrostatic field (CEF) is large and spin-orbit interaction can be treated as a small perturbation, the electron orbitals are firmly coupled to the lattice by CEF and hybridization. The associated orbital moment ($\mathbf{L}$), and through spin-orbit coupling the spin moment ($\mathbf{S}$), are oriented along a well-defined direction, called the easy-direction of magnetization. An applied magnetic field rotates $\mathbf{S}$, but the charge density (depicted as oval shape) remains fixed to the lattice. The change in the value of $\mathbf{L}$ along different magnetization directions results in a weak magnetic anisotropy. (b) In $4f$ systems, as described in the standard model, the spin-orbit coupling is strong and the CEF is weak, so that the charge density rotates (oval shape) with the total angular momentum ($\mathbf{J}$) which is aligned along the magnetization direction. The difference in energy associated with different orientations of the charge density results in a large magnetic anisotropy.

Since the large splittings in the $5d$ states dominate over the small crystal field splittings in the $4f$ states, the latter are difficult to isolate and measure separately by e.g., using inelastic neutron scattering. Moreover, such measurements are not element specific. What is really needed to separate the $4f$ from the $5d$ contribution is an electron shell specific probe such as provided by x ray absorption (XA).

In this Letter, we will determine the energy splitting and non-sphericity of the $4f$ states in EuO using anisotropic x-ray magnetic linear dichroism (AXMLD), i.e., the angular dependence in x-ray magnetic linear dichroism (XMLD) spectra at the $M_{4,5}$ edges ($3d \rightarrow 4f$ transitions). The measurements, which are confirmed by multiplet calculations, show that there is a significant $4f$ anisotropy. It suggests that in the past the influence of the valence character of the $4f$ states on the magnetic anisotropy might have been underestimated.

XMLD spectra are obtained as the difference between XA spectra measured with the magnetization oriented parallel and perpendicular to the linear polarization of the x rays.

Upon rotation of the crystal the XMLD shows an angular dependence with distinctly different spectra observed at different crystallographic directions. It was recently shown for that localized $3d$ transition metal oxides this anisotropy can be of the same size as the XMLD signal itself [6–8]. Here we show that although for rare earths the AXMLD is much smaller, it can never the less be observed and provide novel information.

Motivation to study EuO stems from its fascinating properties and technologically important features for spintronics research [9]. EuO with rock salt structure is an ionic ferromagnetic semiconductor with a bandgap of 1.2 eV and a Curie temperature (T_C) of 69 K [10]. Eu-rich EuO becomes metallic below T_C showing a huge metal-insulator transition (MIT) where the resistivity drops by up to 13 orders of magnitude [11]. An applied magnetic field shifts the MIT temperature, resulting in a colossal magnetoresistance (CMR), which is even larger than in $La_{1-x}Sr_xMnO_3$. Evidence for the spin splitting of the $5d$ conduction band in the ferromagnetic state due to direct exchange interaction with the polarized Eu $4f$ spins comes from the red shift (of 0.3 eV) of the optical absorption edge below T_C. This red shift has recently also been observed using O KLL Auger spectroscopy [12]. Furthermore, free carriers can be introduced by photo doping or field doping of the highly spin polarized conduction band [13]. EuO with its $[Xe]4f^75d^06s^0$ configuration is well-suited for our demonstration. The low in-plane magnetic anisotropy of the ferromagnetic EuO makes it possible to align the magnetization in arbitrary direction using an external field.

For the experiments 500 nm thick single-crystalline EuO films were grown by thermal evaporation of Eu in presence of 3×10^{-9} Torr O_2 on a 1.3 nm SrO buffer layer deposited on top a clean Si(001) surface [14] and capped in situ with 10 nm amorphous Si. The surface near region probed by total electron yield (electron escape depth 5-8 nm [15]) contains 7.5% of Eu_2O_3 that was quantified fitting the experimental data with spectra of the pure compounds [16]. The Eu_2O_3 contribution is due to surface oxidation from the residual oxygen background pressure following the termination of the film growth.

XA spectra were measured in electron yield mode on beamline 4.0.2 at the Advanced Light Source [17] in normal incidence at T=15 K with external fields of 0.5 T by varying the orientation of x-ray linear polarization **E** and external magnetic field **H** relative to the [100] crystalline axes, c.f., inset to Fig. 2(a). The Eu $M_{4,5}$ XA spectrum is shown in Fig. 2(a) and agrees well with previously reported Eu $M_{4,5}$ XA spectra of EuO [16, 18] recognizing the small additional intensity around 1133 eV is due to a 7.5% Eu_2O_3.

4

The XMLD spectrum is defined here as the difference between XA spectra with $\mathbf{H}$ parallel and perpendicular to $\mathbf{E}$, i.e., at angles ϕ and $\phi + 90°$ to the [100] direction,

$$I_{\text{XMLD}}(\phi) = I_{\text{XA}}(\mathbf{H}_\phi, \mathbf{E}_\phi) - I_{\text{XA}}(\mathbf{H}_{\phi+90°}, \mathbf{E}_\phi), \tag{1}$$

where ϕ is the angle with the [100] direction.

For cubic symmetry the angular dependence of the XMLD in the (001) plane is predicted to be [6, 7]

$$I_{\text{XMLD}}(\phi) = \frac{1}{2}\left[(I_0 + I_{45}) + (I_0 - I_{45})\cos 4\phi\right], \tag{2}$$

where $I_0 \equiv I_{\text{XMLD}}(\phi = 0°)$ and $I_{45} \equiv I_{\text{XMLD}}(\phi = 45°)$. The experimental I_0 and I_{45} spectra, which have $\mathbf{E}$ along the [100] and [110] direction, respectively, are shown in Fig. 2(b). Equation (2) shows that all XMLD spectra are a linear combination of these two spectra [7].

The XMLD intensity spans a range of approx. $\pm 15\%$ of the XA near the M_5 edges. This is substantially higher than the XMLD signals observed at the transition metal oxide L_3 edges, which are typically about 5% of the L_3 intensity. On the other hand, only a very weak dependence of the Eu $M_{4,5}$ XMLD signal on the relative orientation of x-ray polarization with respect to the crystal lattice is observed. The most pronounced effect is a small variation in the XMLD spectra near 1156 eV.

To show the angular variation in the XMLD more clearly, we introduce here the residual XMLD spectrum $I_{\text{XMLD}}^{\text{RES}}$ as the measured spectrum with the average XMLD spectrum, $\frac{1}{2}(I_0 + I_{45})$, subtracted,

$$I_{\text{XMLD}}^{\text{RES}}(\phi) \equiv I_{\text{XMLD}}(\phi) - \frac{1}{2}(I_0 + I_{45}) = \frac{1}{2}(I_0 - I_{45})\cos 4\phi, \tag{3}$$

where the right hand side is obtained by substituting Eq. (2). Figure 2(c) shows the measured $I_{\text{XMLD}}^{\text{RES}}$ spectra for $0° \leq \phi \leq 45°$. The results of the modeled angular dependence is displayed by red lines using Eq. (3) with the experimental data for I_0 and I_{45} from Fig. 2(b). Although the angular variation of the XMLD signal is only 1% of the Eu M_5 XA, the experimental data follows very well the expected angular dependence, and is as good as in transition metal oxides [7, 8].

To confirm the anisotropic XMLD signal at the Eu $M_{4,5}$ edges we compare our experimental data with atomic multiplet calculations [15, 19]. Electric-dipole transitions Eu^{2+} $3d^{10}4f^7 \rightarrow 3d^9 4f^8$ were calculated in octahedral symmetry with the specified directions of
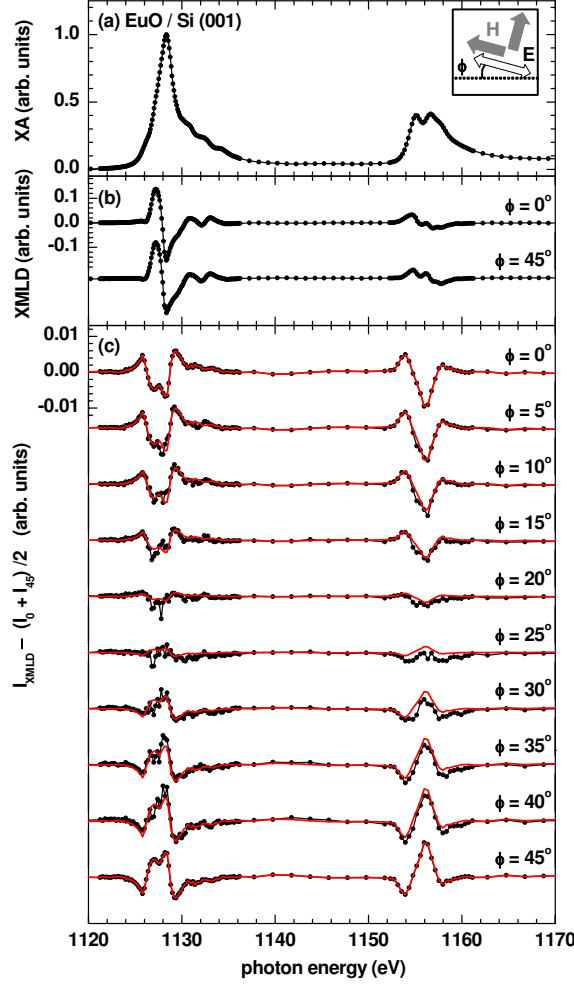
FIG. 2: (Color online) Angular dependence of the Eu $M_{4,5}$ XMLD in EuO/Si(001). (a) XA spectrum averaged over all angles ϕ. (b) XMLD spectra I_0 and I_{45} as measured for $\phi = 0°$ and $\phi = 45°$. The experimental geometry is depicted in the inset of (a)indicating the linear polarization **E** (white arrow) at an angle ϕ to the [100] axis (dashed line) and applied external fields **H** (gray arrows) at angles ϕ and $\phi + 90°$, respectively [c.f., Eq. (1)]. (c) Residual spectra $I_{\mathrm{XMLD}}^{\mathrm{RES}}$ for $0° \leq \phi \leq 45°$. These are the observed XMLD spectra minus the averaged XMLD according to $I_{\mathrm{XMLD}}^{\mathrm{RES}} = I_{\mathrm{XMLD}}(\phi) - \frac{1}{2}(I_0 + I_{45})$. Symbols indicate the experimental data and (red) lines give the modeled angular dependence using the experimental I_0 and I_{45} spectra.

E and **H** using the same atomic parameters as before [20]. Figure 3 shows the calculated I_0 and I_{45} in comparison with experimental data obtained from EuO(001), where the same scaling is used for XMLD and AXMLD spectra. The experimentally observed features are nicely reproduced by the calculation and in quantitative agreement.
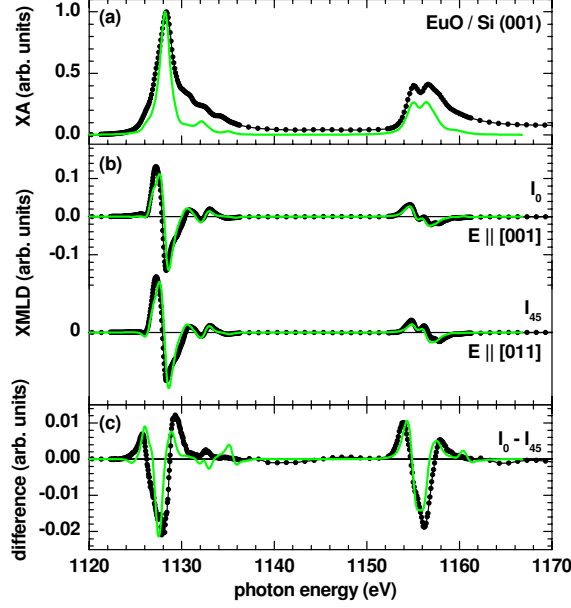
FIG. 3: (Color online) Comparison of experimental Eu $M_{4,5}$ XA and XMLD spectra obtained from EuO/Si(001) (black dots) with results of atomic multiplet calculations (green lines) for V_0^4=0.175 meV. (a) XA spectrum. (b) Fundamental XMLD spectra I_0 (upper spectrum) and I_{45} (lower spectrum). (c) Difference spectrum $I_0 - I_{45}$.

First of all, it is worth noting that the $3d$ core state, which has a binding energy above 1 keV and is spherical symmetric, can not be responsible for the observed angular dependence. If the CEF is zero, then all the f-sublevels are degenerate, making the f level rotationally invariant, so the $3d \rightarrow 4f$ XMLD will be the same at every angle. This is indeed confirmed by the calculations, which show that the XMLD is isotropic for the atomic ground state Eu^{2+} f^7 $^8S_{7/2}$. Hence the only source of the angular dependence is the effective CEF that splits the $4f$ level. Sublevels that have a different energy will have charge densities with distinctly different angular dependencies. The CEF can be written as a multipole expansion over reduced spherical harmonics, where in cubic symmetry the non-vanishing terms give quadrupolar and octupolar contributions quantified by the parameters V_0^4 and V_0^6, respectively [21]. The CEF will be smaller in size than the $4f$ spin-orbit splitting of 0.65 eV and much smaller than the $4f$ Coulomb integrals [20]. The results of the calculations showed that such values of the CEF do not noticeably change the shape and magnitude of the XA and XMCD spectra but only affect the size of the AXMLD. In the specific case of the $4f^7 \rightarrow 3d^9 4f^8$ transition, the shape of the difference spectrum $I_0 - I_{45}$ hardly alters,

and its magnitude is linearly proportional to the value of V_0^4, whereas V_0^6 has a much less influence. This linear dependence allows us to uniquely determine the leading crystal field parameter. A quantitative agreement with the experimental spectra for EuO is obtained for $V_0^4 = 175$ meV [21]. The calculations furthermore show that $I_0 - I_{45}$ does neither depend on the size of the applied exchange field nor on the size of the $4f$ spin-orbit interaction, while scaling the Slater integrals only gives a modest change of the shape and size of $I_0 - I_{45}$. The symmetry, on the other hand, is of major importance and going from octahedral to tetrahedral environment the $I_0 - I_{45}$ spectrum changes sign while roughly maintaining the same shape.

The CEF value of 175 meV obtained by AXMLD is larger than the values quoted for trivalent lanthanides [2, 22], but still an order of magnitude smaller than the crystal field parameters for the $3d$ transition metal oxides. The relatively large value partly reflects the fact that, different to trivalent rare earth ions, the $4f$ shell in Eu^{2+} is not screened by $5d$ electrons, making the ionic atomic radius $\sim 20\%$ larger. Furthermore, apart from the charge potential, the effective energy splitting in the $4f$ includes effects such as hybridization, wave function overlap, band structure, and interaction with the $5d$ states. The experimental evidence for a substantial $4f$ splitting clearly shows that the standard model for rare earths can not be strictly valid and that one needs to take into account the influence of a considerable non-spherical interaction acting on the $4f$ shell. While it has been previously assumed that the $4f$ states should have at least some valence character, and therefore the rotational invariance is broken, using AXMLD we have been able to monitor the angular dependence induced by the $4f$ valence character for the first time directly. Generalizing our results to other rare earths, we might conclude that there is a significant effective CEF which hinders the charge density from following the rotation of the magnetization. This finding has important consequences for the magnetic anisotropy, dynamical processes of spin rotation, and orbital ordering phenomena in rare-earth containing compounds.

To summarize, we have shown that the anisotropy in XMLD at the Eu^{2+} $M_{4,5}$ edges of EuO(001) is very well described with the model developed for cubic transition metal oxides [6–8]. Multiplet calculations show that the size of the anisotropic XMLD for Eu f^7 is proportional to the effective CEF parameter V_0^4. The experimental spectra evidence a significant energy splitting of the f states, where the charge density of each of the sublevels obtains a different angular dependence. This charge asphericity implies that pinning of the

f states by the local environment is a realistic possibility.

───────

[1] L. Smentek and B. G. Wybourne, *TOptical Spectroscopy of Lanthanides: Magnetic and Hyperfine Interactions* (CRC Press, 2007).

[2] R. E. Watson and A. J. Freeman, Phys. Rev. **133**, A1571 (1964).

[3] M. S. S. Brookes and B. Johansson, in *Handbook of Magnetic Materials*, Vol. 7, Ed. K. H. J. Buschow, p. 139, (Elsevier Science, New York, 1993).

[4] P. Bruno, Phys. Rev. B. **39**, 865 (1989).

[5] G. van der Laan, J. Phys.: Condens. Matter **10**, 3239 (1998).

[6] A. A. Freeman *et al.*, Phys. Rev. B **73**, 233303 (2006).

[7] E. Arenholz *et al.*, Phys. Rev. B **74**, 94407 (2006).

[8] E. Arenholz *et al.*, Phys. Rev. Lett. **98**, 197201 (2007).

[9] A. Mauger and C. Godart, Phys. Rep. **141**, 51 (1986).

[10] B. T. Matthias, R. M. Bozorth, and J. H. van Vleck, Phys. Rev. Lett. **7**, 160 (1961).

[11] G. Petrich, S. von Molnr, and T. Penney, Phys. Rev. Lett. **26**, 885 (1971).

[12] P. G. Steeneken *et al.*, Phys. Rev. Lett. **88**, 047201 (2002).

[13] E. L. Nagaev, Phys. Stat. Sol. (b) **145**, 11 (1988).

[14] J. Lettieri *et al.*, Appl. Phys. Lett. **83**, 975 (2003).

[15] B. T. Thole *et al.*, Phys. Rev. B **32**, 5107 (1985).

[16] E. Negusse *et al.*, J. Appl. Phys. **99**, 08E507 (2006).

[17] A. T. Young *et al.*, J. Synchrotron Rad. **9**, 270 (2002).

[18] H. Ott *et al.*, Phys. Rev. B **73**, 094407 (2006).

[19] J. B. Goedkoop *et al.*, Phys. Rev. B **37**, 2086 (1988).

[20] The Hartree-Fock values of the Slater parameters, before reduction to 80%, (Ref. [15]) are for Eu f^7: F^2=13.00, F^4=8.11, F^6=5.82, ζ_f=0.16 and for Eu $3d^9 4f^8$ ($4f$-$4f$): F^2=13.79, F^4=8.62, F^6=6.19, and ($3d$-$4f$): F^2=11.24, F^4=8.75, F^6=4.04, G^1=6.15, G^3=3.60, G^5=2.49, ζ_f=0.19, ζ_d=11.24 (all in eV). The $3d$ spin-orbit interaction is scaled to 98.53%. The intrinsic

lifetime broadening is taken as a Lorentzian with Γ=0.25 (0.5) eV for the M_5 (M_4) edge and the instrumental broadening included as a Gaussian with σ=0.25 eV.

[21] The CEF with V_0^4=1 eV splits a one-electron f state in octahedral symmetry into levels A_2 [f_{xyz}], T_2 [$f_{x(z^2-y^2)}$, $f_{y(x^2-z^2)}$, $f_{z(x^2-y^2)}$], and T_1 [$f_{x(5x^2-3r^2)}$, $f_{y(5y^2-3r^2)}$, $f_{z(5z^2-3r^2)}$] with energies $-2/3$, $-1/9$, and $1/3$ eV, respectively.

[22] J. B. Gruber, B. Zandi, and L. Merkle, J. Appl. Phys. **83**, 1009 (1998).